Torque ripple reduction in a surface permanent magnet synchronous machine with stator inter-turn short circuit

Elmehdi Bahri[1,2], **Remus Pusca**[1], **Raphael Romary**[1], **Driss Belkhayat**[2]

1. Univ. Artois, EA 4025, LSEE, 62400 Béthune, France
LSEE Faculté des Sciences Appliquées, Technoparc Futura, 62400 Bethune, France
raphael.romary@univ-artois.fr

2. LSET, Cadi Ayyad University,
BP 549, av. Abdelkarim Elkhattabi, Gueliz, Marrakech, Morocco
dbelkhayat@gmail.com

ABSTRACT. *This paper presents a modeling of a surface mounted permanent magnet synchronous motor in healthy and faulty cases and a control approach aiming at reducing the torque ripple which appears in faulty case. The fault considered in this work is a stator inter-turn short circuit. The model proposed in this paper is based on the dynamic equations of the motor. Simulation results show the possibility to reduce the torque ripple by according the motor supply control in concordance of incipient faults or motor asymmetry.*

RÉSUMÉ. *Cet article présente une modélisation de la machine synchrone à aimants permanents montés en surface, en cas sain et en cas de défaut de court-circuit entre spires statoriques, en vue de réduire les ondulations de couple générés par le défaut. Le modèle proposé est basé sur les équations dynamiques du moteur. Les simulations montrent la possibilité de réduire les ondulations de couple en modifiant l'alimentation.*

KEYWORD: *synchronous motor, torque ripples, stator short circuit, dynamic modeling.*

MOTS-CLÉS : *moteur synchrone, ondulations de couple, court-circuit statorique, modélisation dynamique.*

DOI:10.3166/EJEE.18. 293-317 © Lavoisier 2016

Extended abstract

☛ The work presented in the paper aims at developing a methodology to reduce the torque ripples generated by a stator inter-turn short circuit in a surface permanent magnet synchronous machine. The harmonic torque components generated by the fault have been identified and the inverse current component to be injected in the supply currents has been determined to reduce the main torque component, which is at twice the supply frequency. The approach that have been used to determine this inverse current component is based on the analytical calculation of the air gap flux magneto-motive force that takes into account the magnetic effect of the currents in each slot. Another approach is based on circuit equations and require the knowledge of the inductances in healthy and in faulty condition to implement the correction principle in matlab-simulink simulations. These simulations give convincing results when the machine operates in speed-control operating conditions. Experimental tests have been realized to validate the theoretical study. The used test bench includes a Permanent Magnet Synchronous Machine (PMSM) coupled to a DC machine. The PMSM is powered by an inverter controlled by a Dspace system able to tune the inverse current component and ensure the vector control. A properly positioned accelerometer is used to measure the tangential vibrations generated by torque fluctuations. For the considered fault, the reduction of the harmonic of tangential vibrations at twice the supply frequency was demonstrated by injection of an inverse current component. A good agreement between theory and experimentation in terms of the amplitude of the inverse component is obtained.

1. Introduction

Surface Permanent Magnet Synchronous Motors (SPMSM) are widely used in various applications, such as industry, electric vehicles, airplanes, etc ... As mentioned by Li *et al.* (2012) and Borghi *et al.* (1998), the advantages of these machines in these applications is their high performance, high torque density, robust construction, and non-use of brushes. However, Mademlis and Margaris (2002), Abdel-Rady (2007), and Pellegrino *et al* (2010), have shown that the torque ripple generated by SPMSM and rotor iron losses are factors that degrade its use and decrease the efficiency.

Jeong *et al*. (2013) have shown that faults in electric motor as winding dissymmetry, demagnetization of the rotor, short circuit between turns or eccentricity, leads to increase torque ripples and also the losses. The degradation can cause problems to the operational continuity if the control is not adjusted, taking account the defect. This is true for applications such as those related to electric vehicles and aeronautic systems, where a high reliability of the machine is required.

Reducing torque ripple in a healthy synchronous motor has been the subject of several research and different strategies have been proposed. The best known is to

control the stator currents to compensate the torque ripple. As proposed by Favre *et al.* (1993), the currents are calculated by several methods, some of them uses the decomposition of the electromotive force to determine a limited number of current harmonics while others use the finite element method to get the current waveforms. Holtz and Springob (1996) uses another approach based on the analytical modelling of the machine to determine the harmonic currents with verification of an optimization criterion.

In the case of a faulty synchronous motor, many works have been performed for its modelling and control. One of the adopted methods is based on dynamic modelling of the faulty machine using mathematical equations of flux, voltages and currents which are separated in direct and inverse components as done by Jeong *et al* (2013). In this work, the objective of the control strategy is based on the cancellation of the negative sequence of the currents, using two controllers.

The aim of this paper is to define a control method able to cancel the torque harmonics generated by a stator inter-turn short circuit in a SPMSM. The paper is organized as follows: the second section presents the developed SPMSM model used to study the current and the torque in healthy and faulty case. In the third section the simulation principle used to model the healthy and faulty SPMSM in Matlab/Simulink environment is detailed. In the fourth section the mathematical approach developed to calculate the current references which lead to reduce torque ripple is presented. Simulation results and discussions are presented in the fifth section, and the sixth section is devoted to the experimental tests.

2. SPMSM Modeling

The SPMSM considered in this paper has a smooth rotor and its number of pole pairs is p=2. The stator phase winding is composed of six elementary coils, and the inter-turn short circuit fault is assumed to occur in the first elementary coil of the phase a. The chosen SPMSM model is similar as this used by Vaseghi *et al* (2011). It is based on a three-phase dynamic model using the electrical equivalent circuit, which does not take into account the iron losses and saturation.

Thanks to this model it is possible to introduce a fault by adapting the different machine parameters for each phase. Figure 1 shows the used SPMSM model. The different elements presented in Figure 1 are:

L_s : self inductance.

M : mutual inductance.

L_{af} : self inductance of faulty winding af.

M_{afa2} : mutual inductance between windings af and a2.

M_{a2b} : mutual inductance between windings a2 and b.

M_{a2c} : mutual inductance between windings a2 and c.

M_{afb} : mutual inductance between windings af and b.

M_{afc} : mutual inductance between windings af and c.

R_f : fault resistance.

i_f : fault current.

V_a : voltage of phase a.

V_b : voltage of phase b.

V_c : voltage of phase c.

V_N : voltage of neutral point.

As the rotor is assumed to be smooth, all the inductances do not depend on the rotor position and they are constant.

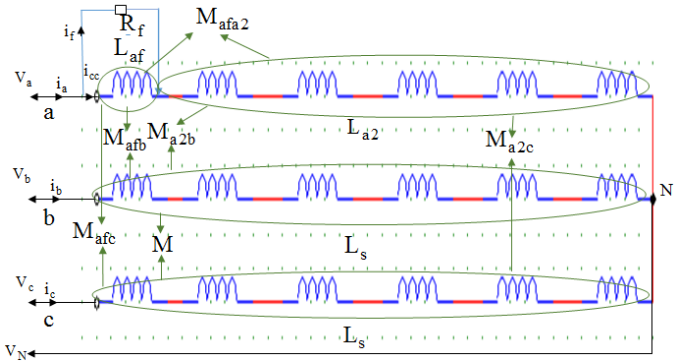

Figure 1. SPMSM model for short circuit inter turn fault

2.1. Electrical equations

2.1.1. Healthy machine

For the considered model in healthy case, the stator voltages are given by (1) and (2):

$$\begin{bmatrix} V_{aN} \\ V_{bN} \\ V_{cN} \end{bmatrix} = \begin{bmatrix} R_s & 0 & 0 \\ 0 & R_s & 0 \\ 0 & 0 & R_s \end{bmatrix} \begin{bmatrix} i_a \\ i_b \\ i_c \end{bmatrix} + \frac{d}{dt} \begin{bmatrix} \Psi_{ra} \\ \Psi_{rb} \\ \Psi_{rc} \end{bmatrix} + \begin{bmatrix} L_s & M & M \\ M & L_s & M \\ M & M & L_s \end{bmatrix} \times \frac{d}{dt} \begin{bmatrix} i_a \\ i_b \\ i_c \end{bmatrix} \quad (1)$$

$$i_a + i_b + i_c = 0 \tag{2}$$

$\Psi_{ra}, \Psi_{rb}, \Psi_{rc}, R_s$ are respectively the sinusoidal fluxes through winding a, b, c generated by the rotor and the phase resistance. This expression is obtained considered the development presented in appendix 2.

The potential of the neutral point can vary in the presence of the fault. Therefore it is necessary to use the equations of voltage without the introduction of the neutral point potential. The voltage equations can then be reduced to two equations (3) independent of the neutral point potential.

$$\begin{bmatrix} V_a - V_b \\ V_a - V_c \end{bmatrix} = \begin{bmatrix} R_s & -R_s \\ 2R_s & R_s \end{bmatrix} \begin{bmatrix} i_a \\ i_b \end{bmatrix} + \frac{d}{dt} \begin{bmatrix} \Psi_{ra} - \Psi_{rb} \\ \Psi_{ra} - \Psi_{rc} \end{bmatrix} + \begin{bmatrix} L_s - M & M - L_s \\ 2L_s - 2M & L_s - M \end{bmatrix} \times \frac{d}{dt} \begin{bmatrix} i_a \\ i_b \end{bmatrix} \tag{3}$$

2.1.2. Faulty machine

The electrical equations of three-phase faulty SPMSM in the abc reference obtained from (1a) and (2a) presented in appendix 2 can be expressed as (4) and (5):

$$\begin{bmatrix} V_{aN} \\ V_{bN} \\ V_{cN} \\ 0 \end{bmatrix} = \begin{bmatrix} R_s & 0 & 0 & -R_{af} \\ 0 & R_s & 0 & 0 \\ 0 & 0 & R_s & 0 \\ -R_{af} & 0 & 0 & R_{af} + R_f \end{bmatrix} \begin{bmatrix} i_a \\ i_b \\ i_c \\ i_f \end{bmatrix} + \frac{d}{dt} \begin{bmatrix} \Psi_{ra} \\ \Psi_{rb} \\ \Psi_{rc} \\ -\Psi_{raf} \end{bmatrix} + \begin{bmatrix} L_s & M & M & -L_{af} - M_{afa2} \\ M & L_s & M & -M_{afb} \\ M & M & L_s & -M_{afc} \\ L_{af} + M_{afa2} & M_{afb} & M_{afc} & -L_{af} \end{bmatrix} \times \frac{d}{dt} \begin{bmatrix} i_a \\ i_b \\ i_c \\ i_f \end{bmatrix} \tag{4}$$

$$i_a + i_b + i_c = 0 \tag{5}$$

Where Ψ_{raf}, Ψ_{ra2} are respectively the sinusoidal fluxes through windings af, a2, and R_{af} is the resistance of faulty winding af.

As done before for the healthy SPMSM, the neutral point potential can be removed from (4) and (5) to obtain (6):

$$\begin{bmatrix} V_a - V_b \\ V_a - V_c \\ 0 \end{bmatrix} = \begin{bmatrix} R_s & -R_s & -R_{af} \\ 2R_s & R_s & -R_{af} \\ -R_{af} & 0 & R_{af} + R_f \end{bmatrix} \begin{bmatrix} i_a \\ i_b \\ i_f \end{bmatrix} + \frac{d}{dt} \begin{bmatrix} \Psi_{ra} - \Psi_{rb} \\ \Psi_{ra} - \Psi_{rc} \\ -\Psi_{raf} \end{bmatrix} + \begin{bmatrix} L_s - M & M - L_s & -L_{af} - M_{afa2} + M_{afb} \\ 2L_s - 2M & -M - L_s & -L_{af} - M_{afa2} + M_{afc} \\ L_{af} + M_{afa2} - M_{afc} & M_{afb} - M_{afc} & -L_{af} \end{bmatrix} \times \frac{d}{dt} \begin{bmatrix} i_a \\ i_b \\ i_f \end{bmatrix} \quad (6)$$

2.2. Electromagnetic torque

The electromagnetic torque expression is calculated with the product between the fluxes derivative and the currents.

$$C_e = \frac{1}{2} \begin{bmatrix} (\frac{d}{d\theta}\Psi_{ra2}) \times i_a + (\frac{d}{d\theta}\Psi_{rb}) \times i_b \\ + (\frac{d}{d\theta}\Psi_{rc}) \times i_c + (\frac{d}{d\theta}\Psi_{raf}) \times (i_a - i_f) \end{bmatrix} \quad (7)$$

2.3. Mechanical equation

The SPMSM mechanical behavior is expressed by:

$$J\frac{d\Omega}{dt} = C_e - fr\Omega - C_r \quad (8)$$

with:

- J : moment of inertia.
- C_e : electromagnetic torque.
- C_r : constant torque.
- fr : friction coefficient.
- Ω : rotation angular speed.
- $\theta = \int \Omega dt$: rotor angular position.

In the simulation, it will be considered that the torque Cr is null.

2.4. parameters

The determination of the SPMSM parameters in the healthy and faulty case is based on the method presented by Hamiti *et al*. (2010), that uses the magnetomotive force (mmf) generated by the stator winding in healthy and faulty case to calculate the inductance. The following relationship is used:

$$L_{xy} = \mu_0 RL \int_0^{2\pi} N_x(\alpha_s) N_y(\alpha_s) e^{-1}(\alpha_s) d\alpha_s \tag{9}$$

where:

L_{xy} : the self inductance (x=y), mutual inductance (x≠y) between windings x and y.

μ_0 : permeability of vacuum.

R : the radius of the stator.

L : the length of the slots.

$N_x(\alpha_s)$, $N_y(\alpha_s)$: respectively the magnetomotive force of windings x and y flowed by a unit current.

e : thickness of the air gap.

α_s : the angular abscissa of a point in the air gap in a stator reference.

The values of inductances calculated analytically in healthy and faulty case are given in Table 1. The considered machine is a 230/400V, 3kW, 5A, 20Nm, 4 poles, 50Hz synchronous machine that will be used in further study for experimental validation. The appendix 1 A gives the parameters value used to calculate the inductances with (9). In this paper, the fault of the stator winding is generated by an inter-turns short of 16.66% of the number of turns in phase a.

Table 1. Inductances and resistances of studied SPMSM calculated analytically in (a) healty and (b) faulty case

L_s (H)	M (H)	R_s (Ω)
0.0746	-0.0312	3.6

(a)

L_s (H)	M (H)	L_{af} (H)	L_{a2} (H)	M_{afa2} (H)	$M_{afb} = M_{afc}$ (H)	R_s (Ω)	R_{af} (Ω)
0.0746	-0.0312	0.00569	0.0064	0.0056	-0.0052	3.6	0.6

(b)

3. Simulation principle of healthy and faulty machine

The bloc diagram of the simulation principle is presented in Figure 2. Here the electromagnetic torque is determined from the rotor flux and stator currents. The rotor position is calculated from the mechanical equation. The rotor flux is

expressed as a function of the rotor position angle from recording tables. The currents supplying the SPMSM are obtained from electrical equations.

The rotor flux values stored in recording tables for each phase are obtained from integration of electromotive forces which can be identified practically in alternator running mode.

The effect of the currents on the torque ripple is analyzed considering a control loop to regulate the supply currents. This control loop is shown in Figure 3, where i_{ar}, i_{br}, i_{cr} are calculated through the Corrected Current Reference (CCR) block introduced in the next section (see Figure 5).

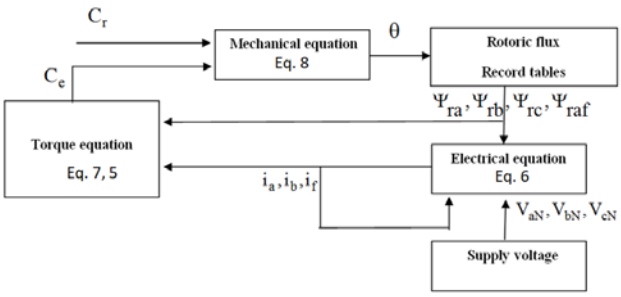

Figure 2. Block diagram of the SPMSM model used in simulation

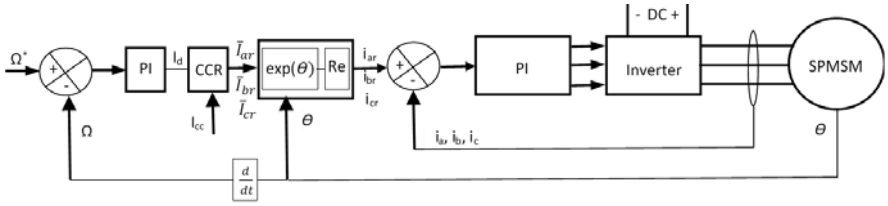

Figure 3. PMSM control loop

4. Torque ripple reduction approach for faulty SPMSM

It is well known that a stator inter-turn short circuit induces torque ripple at twice the supply frequency and reduces the average torque, as demonstrated by Jeong *et al.* (2013) and Tallam *et al.* (2002). The torque harmonic component at twice of supply frequency mainly provides from the stator inverse sequence space harmonics mmf at h = -2 and by the fundamental rotor space harmonics flux density as shown in Bahri *et al.* (2017) and Bahri *et al.* (2014). So to reduce this torque harmonic it is necessary to cancel the mmf at h=-2 for the considered machine with 2 pole pairs. The method used for the reduction of torque ripple is performed by an analytical approach. First the mmf is calculated for faulty SPMSM, and then the analytical

method is developed to cancel the negative sequence of faulty SPMSM mmf. This is done by injection of an inverse current of rms value I_i in the current references as shown by Bahri *et al*. (2016).

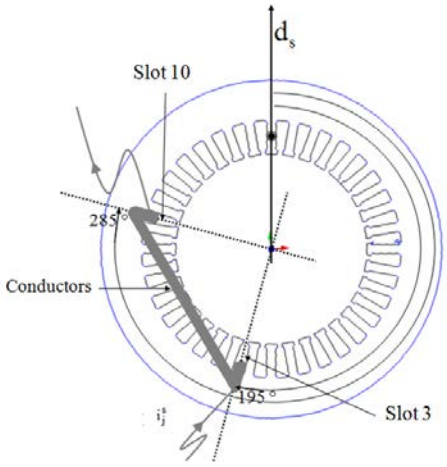

Figure 4. Elementary faulty coil configuration in the stator yoke

A stator elementary coil where the short-circuit fault occurs (Figure 1) is presented in Figure 4. It is composed of two beams; one of them has a side inserted into the slot 3 and the other side inserted into the slot 10.

The rank h of space harmonic mmf ε_h^s generated by all SPMSM slot conductors flowed through by a current of I_j^s rms value obtained as detailed by Bahri *et al* (2017) is given in complex notation by:

$$\underline{\varepsilon}_h^s = \sum_{j=1}^{N_t^s} \frac{n_j^e I_j^s}{\sqrt{2}(\pi-\delta)h} \Gamma_h e^{j(h\beta_j^s+\varphi_j)} \tag{10}$$

with:

$$\Gamma_h = \frac{\sin[h(1-r_d^s)\pi/N_t^s]}{h(1-r_d^s)\pi/N_t^s}$$

where:

d_s : stator reference axis.

h : mmf space harmonic rank.

n_j^e : number of conductors in stator slot.

δ : half slot width $\delta = (1 - r_d^s)\pi / N_t^s$.

l_e^s : stator slot width.

l_d^s : stator tooth width.

r_d^s : stator toothing ratio $r_d^s = l_d^s/(l_d^s + l_e^s)$.

β_j^s : angular position of the stator slot j.

φ_j : current phase angle in the slot j.

N_t^s : total stator slot number.

I_j^s : rms current across the conductors of slot j.

The SPMSM is assumed to be supplied with sine currents. The strategy for calculation of stator currents to decrease the space harmonic stator mmf at h = -2 in the case of a stator inter-turn short circuit in one phase winding is performed using the complex notation of the mmf components. The computation of a mmf space harmonic component is done by considering the currents in each individual slot.

The stator winding mmf at h=-2 is computed in two cases:

– healthy stator winding supplied by direct current of I_d rms value, in this case the mmf harmonic at h=-2 is null*:*

$$\underline{\varepsilon}_{d\text{-}2}^{s} = \sum_{\substack{j=1 \\ j\neq 3,10}}^{N_t^s} \frac{n_j^e I_d}{\sqrt{2}(\pi-\delta)(-2)} \Gamma_{-2} e^{j(-2\beta_j^s + \varphi_{dj})} + \sum_{j=3,10} \frac{n_j^e I_d}{\sqrt{2}(\pi-\delta)(-2)} \Gamma_{-2} e^{j(-2\beta_j^s + \varphi_{dj})} = 0 \quad (11)$$

– faulty stator winding supplied by direct current of I_d rms value:

$$\underline{\varepsilon}_{d-2(fault)}^{s} = \sum_{\substack{j=1 \\ j\neq 3,10}}^{N_t^s} \frac{n_j^e I_d}{\sqrt{2}(\pi-\delta)(-2)} \Gamma_{-2} e^{j(-2\beta_j^s + \varphi_{dj})} + \sum_{j=3,10} \frac{n_j^e I_{cc}}{\sqrt{2}(\pi-\delta)(-2)} \Gamma_{-2} e^{j(-2\beta_j^s + \varphi_{ccj})} \quad (12)$$

where I_{cc} is the rms value of the current in the coil where occurs the inter-turn short circuit (Figure 4).

For the stator winding supplied by inverse current of I_i rms value, it is supposed that the inverse current does not flow through the fault resistance R_f, the stator winding mmf at h=-2 can be expressed as follows:

$$\bar{\varepsilon}^{s}_{i-2\,(fault)} = \sum_{j=1}^{N_t^s} \frac{n_j^e \overline{I_i}}{\sqrt{2}(\pi-\delta)(-2)} \Gamma_{-2} e^{j(-2\beta_j^s+\varphi_{ij})} \tag{13}$$

To cancel the harmonic h = -2, the mmf generated by the inverse and direct current must satisfy the following equation:

$$\bar{\varepsilon}^{s}_{i-2(fault)} = \bar{\varepsilon}^{s}_{d-2} - \bar{\varepsilon}^{s}_{d-2(fault)} \tag{14}$$

Then it comes:

$$\bar{\varepsilon}^{s}_{i-2_{(fault)}} = \sum_{j=3,10} \frac{n_j^e}{\sqrt{2}(\pi-\delta)(-2)} \Gamma_{-2} (I_d e^{j(-2\beta_j^s+\varphi_{dj})} - I_{cc} e^{j(-2\beta_j^s+\varphi_{ccj})})$$

Replacing $\varepsilon^{s}_{i-2\,(fault)}$ with (13), it comes:

$$\begin{aligned} &\sum_{j=1}^{N_t^s} \frac{n_j^e \overline{I_i}}{\sqrt{2}(\pi-\delta)(-2)} \Gamma_{-2} e^{j(-2\beta_j^s+\varphi_{ij})} = \\ &\sum_{j=3,10} \frac{n_j^e}{\sqrt{2}(\pi-\delta)(-2)} \Gamma_{-2} (I_d e^{j(-2\beta_j^s+\varphi_{dj})} - I_{cc} e^{j(-2\beta_j^s+\varphi_{ccj})}) \end{aligned} \tag{15}$$

Finally, after simplification the relationship between the direct current and the inverse current used to compensate the harmonic of rank h=-2 is given by:

$$\overline{I_i} = \frac{I_d \sum_{j=3,10} e^{j(-2\beta_j^s+\varphi_{dj})} - I_{cc} \sum_{j=3,10} e^{j(-2\beta_j^s+\varphi_{ccj})}}{\sum_{j=1}^{N_t^s} e^{j(-2\beta_j^s+\varphi_{ij})}} \tag{16}$$

To simplify (16), it is put in following form where A, B and C are complex quantities:

$$\overline{I_i} = \frac{I_d B - I_{cc} A}{C} \tag{17}$$

and:

$$A = \sum_{j=3,10} e^{j(-2\beta_j^s + \varphi_{ccj})} \; , B = \sum_{j=3,10} e^{j(-2\beta_j^s + \varphi_{dj})} \; , C = \sum_{j=1}^{N_r^s} e^{j(-2\beta_j^s + \varphi_{ij})}$$

Equation (17) is used to obtain the corrected current that leads to decrease the mmf space harmonic of rank h=-2, and therefore to reduce the torque ripple at twice the supply frequency.

In Figure 5 the computation method of the corrected reference current able to decrease the torque ripple is presented. To validate this control strategy, first a direct balanced currents system of I_d rms value and f frequency is considered. The inverse current $\overline{I_i}$ is given by (17), and the reference currents $\bar{I}_{ar}, \bar{I}_{br}, \bar{I}_{cr}$ to cancel torque ripple at 2f are calculated. Finally the time current references i_{ar}, i_{br}, i_{cr} are reconstructed. In following expressions "a" is a complex number: $a = e^{j2\pi/3}$. For current reference calculation, I_{cc} is considered as a known constant rms value. In healthy conditions $I_{cc} = I_i = 0$ and there is only a direct current system I_d and $I_a = I_b = I_c = I_d$.

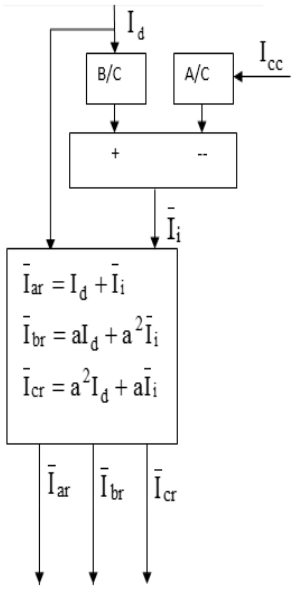

Figure 5. Diagram computation of corrected currents reference

5. Simulation results

The motor model with specific parameters presented in appendix 1 was implemented in Matlab/Simulink. Each stator winding consists of six elementary

coils. A short-turn fault is introduced into the first elementary section located in the winding phase A (Figure 1). To analyze the impact of the current on the torque improvement, the motor supplied by a 50Hz current balanced system in healthy and faulty case, is compared with the case where the currents are adjusted using (17). In simulation, the PWM inverter is modeled by a gain block so, its hashing effect in the current is masked. The simulations are performed at no load, and in stationary operating condition, therefore only the friction torque is imposed to the machine.

5.1. Healthy SPMSM supplied by balanced currents

In Figures 6, 7 and 8, the currents (references + regulated current), electromagnetic torque, and the speed are shown. It can be noticed that the currents make a balanced direct system of 2A peak value, and follow the references with a negligible error. It can be observed that the electromagnetic torque, and the speed are constant without ripple.

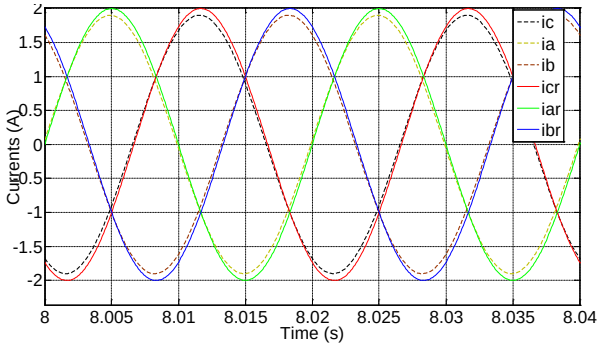

Figure 6. Balanced stator currents supplying the healthy SPMSM: reference and supply currents.

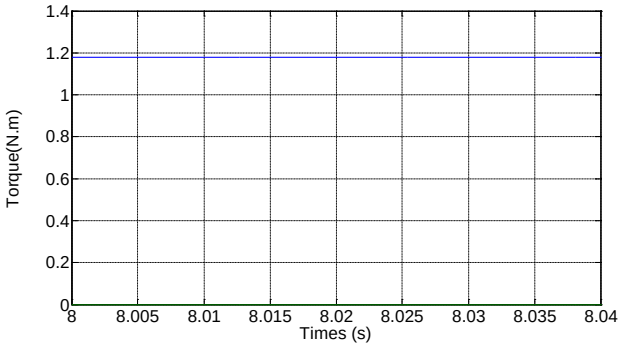

Figure 7. Electromagnetic torque variation for healthy SPMSM supplied by balanced currents.

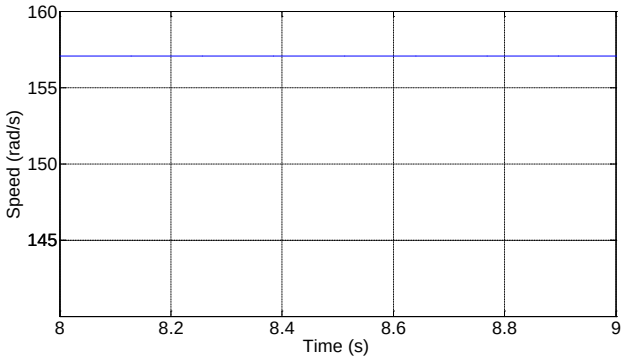

Figure 8. Speed variation for the healthy SPMSM supplied by balanced currents

5.2. Faulty SPMSM supplied by balanced currents

In Figures 9, 10, 11, 12, the supply currents, short-circuit current, electromagnetic torque, and the speed are given respectively in the case of faulty SPMSM supplied by balanced currents. It can be noticed that the short-circuit current has a peak value of 14A and the same frequency as the supply currents. It appears that the electromagnetic torque, and the speed are non-constant with ripples at 100Hz.

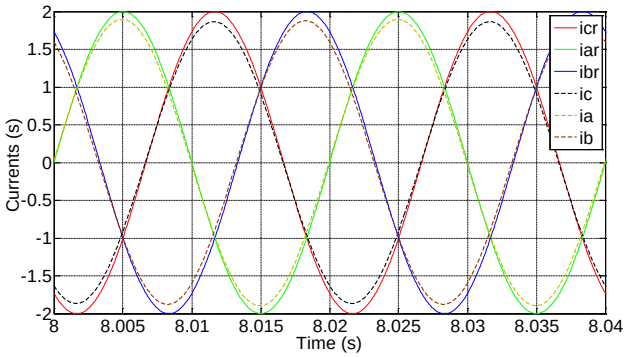

Figure 9. Balanced stator currents supplying the faulty SPMSM: the reference and supply current

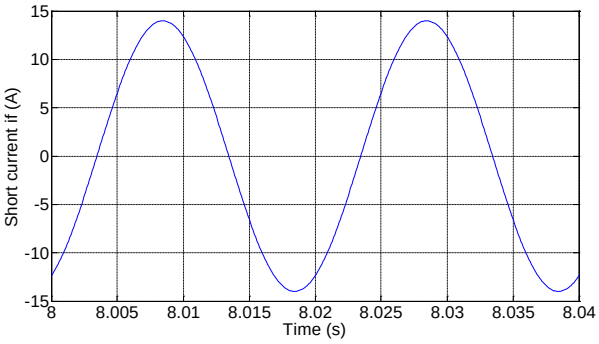

Figure 10. Short-turns current of the faulty SPMSM supplied by balanced currents

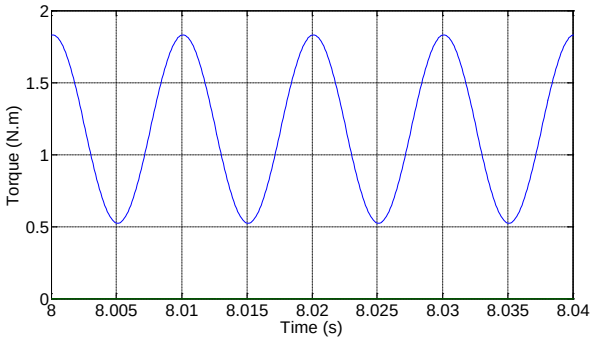

Figure 11. Electromagnetic torque variation for faulty SPMSM supplied by balanced currents.

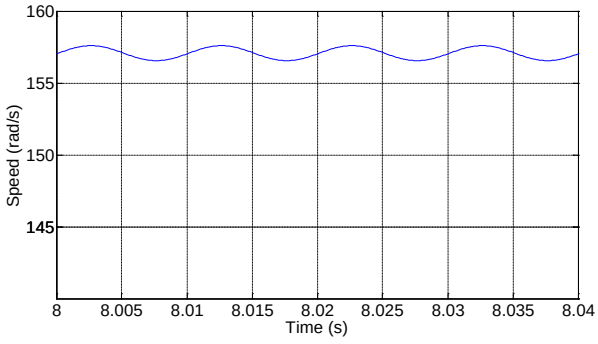

Figure 12. Speed variation for faulty SPMSM supplied by balanced currents

5.3. Faulty SPMSM supplied by corrected currents

Equation (17) leads to an inverse current of I_i =0.75A peak value. In Figures. 13, 14, 15, 16, the supply currents, the shorted-turns current, the electromagnetic torque, and the speed are shown respectively in the case of faulty SPMSM supplied by corrected currents. It clearly appears that the currents make a strong unbalanced system. The short-turns current still has a peak value of 14A and the same frequency as the supply currents. Compared to the case of the faulty SPMSM supplied by balanced currents, the electromagnetic torque and the speed still have ripples at 100Hz. Actually, the torque ripple is not fully cancelled; this is due to the assumption made for calculation of the inverse current where it is considered that the inverse current does not flow through the fault resistance R_f .

Table 2 presents a summary of the results for each of the three cases. It can be noticed that in the case of faulty SPMSM supplied by the corrected currents the electromagnetic torque and speed ripple at 100 Hz are strongly reduced than the case of faulty SPMSM supplied by a balanced currents.

Table 2. Summary of simulation results

	Healthy SPMSM supplied by balanced currents	Faulty SPMSM supplied by balanced currents	Faulty SPMSM supplied by corrected currents
I_a (A)	1.9	1.9	2.32
I_b (A)	1.9	1.87	2.4
I_c (A)	1.9	1.88	1.13
I_d (A)	1.9	1.89	2
I_i (A)	0	0	0.75
φ_a (°)	0	0	0
φ_b (°)	240	240	207.2
φ_c (°)	120	120	99.18
I_{cc} (A)	0	14	14
φ_{cc} (°)	0	63.7	42.85
C_{aver} (N.m)	1.17	1.17	1.17
ΔC (N.m)	0	1.3	0.12
Ω_{aver} (rad/s)	157.08	157.08	157.08
$\Delta\Omega$ (rad/s)	0	1.04	0.1

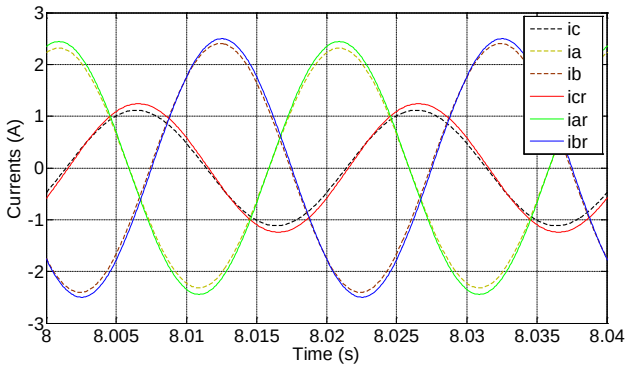

Figure 13. Corrected stator currents for the faulty SPMSM: the reference and supply current.

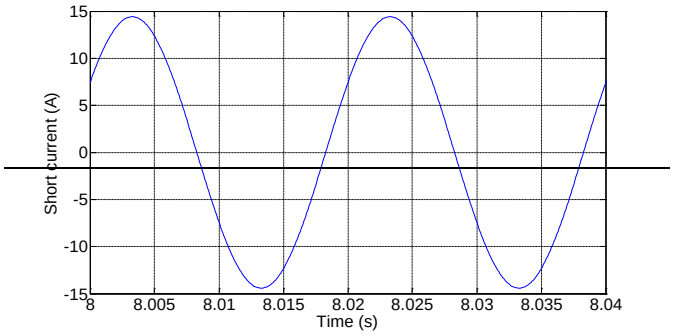

Figure 14. Short-turns current of the faulty SPMSM supplied by corrected currents

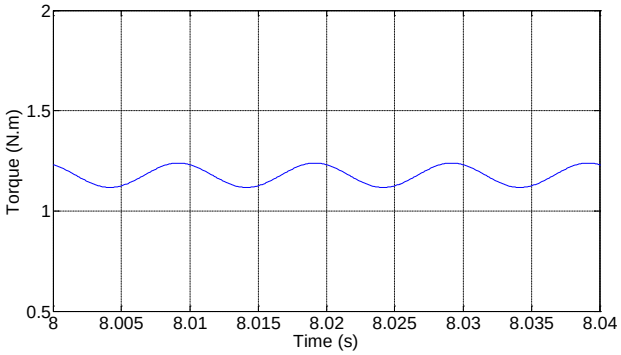

Figure 15. Electromagnetic torque variation of the faulty SPMSM supplied by corrected currents

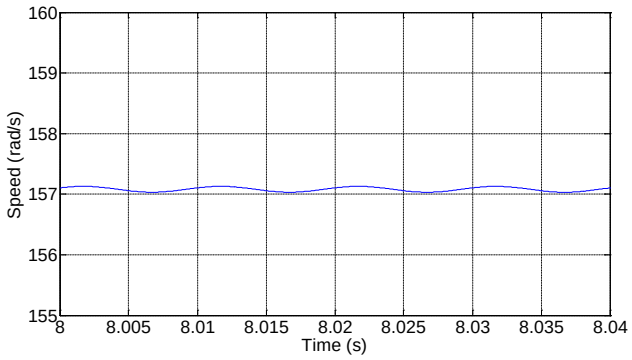

Figure 16. Speed variation of the faulty SPMSM supplied by the corrected currents

6. Experimental results

6.1. Test bench presentation

Experimental tests are performed on a laboratory test bench. A block diagram of the test bench is presented in Figure 17, and a picture shows the machine in Figure 18. The used SPMSM is the same machine that the one studied in the theoretical analysis with the following electrical characteristics: 4.4 kW rated power, 1500 rpm rated speed, 4-pole. The stator winding is composed of three elementary sections per pole per phase that can be individually short-circuited (see Figure 19). The short circuit current is limited through an external rheostat. The machine is fed by an inverter controlled by a dSpace (DS1104) system encoded with simulink that enable to control the currents from a speed reference and from a reference of the inverse current that can be adjusted in magnitude and in phase. The current is regulated by hysteresis controller implemented in the dSPACE system. The torque is not directly measured but the presence of torque harmonics is assessed through the tangential vibrations they generate. An accelerometer with $0.01 mV/mms^{-2}$ sensitivity is suitably placed in order to measure the tangential vibrations of the machine. It is connected to a frequency analyzer (Brüel&Kjær 3560).

The aim of the experiments is to assess the impact of the inverse current component reference current on the reduction of the tangential vibrations at twice the supply frequency generated by the faulty SPMSM. The considered fault is, according to the theoretical analysis, a short circuit a full elementary section located in phase A (Figure 19), with a short-circuit current of 14A peak value

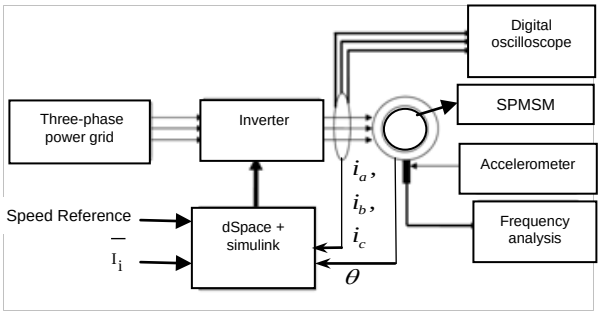

Figure 17. Block diagram of the test bench

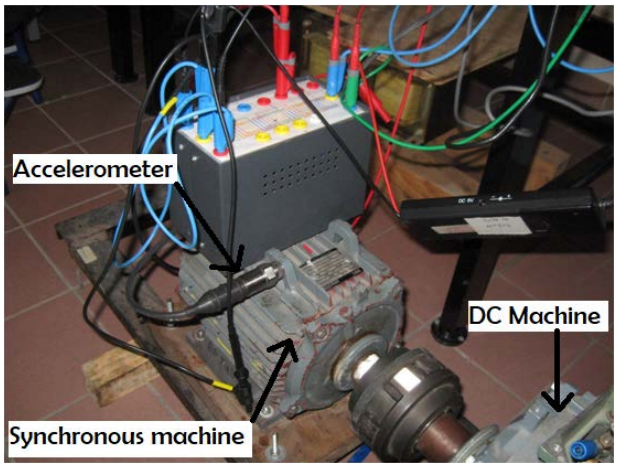

Figure 18. The tested SPMSM

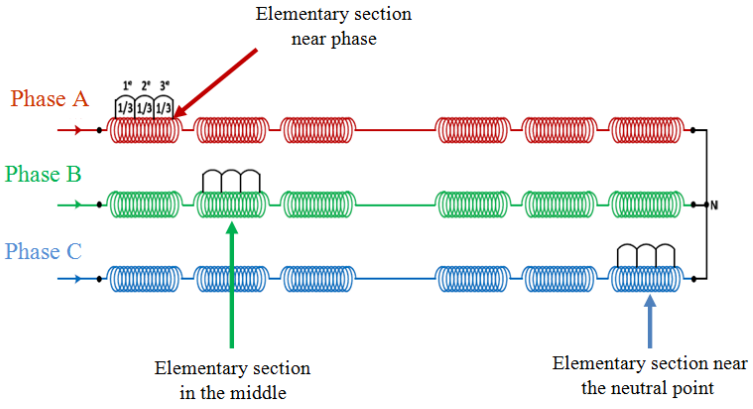

Figure 19. Stator winding connection

6.2. vibration reduction

First, the healthy machine is supplied by a sine three phase current system at 1500rpm-50Hz and 2A peak value. The FFT of the measured tangential vibration is given in Figure 20. Despite the machine operates in healthy conditions, one can observe the presence of vibration spectral lines at 25 Hz, 50 Hz, and 75 Hz, and at higher frequeny that can be justified by eccentricity or rotor demagnetization as reported by Ebrahimi and Faiz (2012), Ebrahimi *et al.* (2014) and Urresty *et al*. (2013). However the harmonic at 100Hz is very low (0.35mV delivered by the accelerometer).

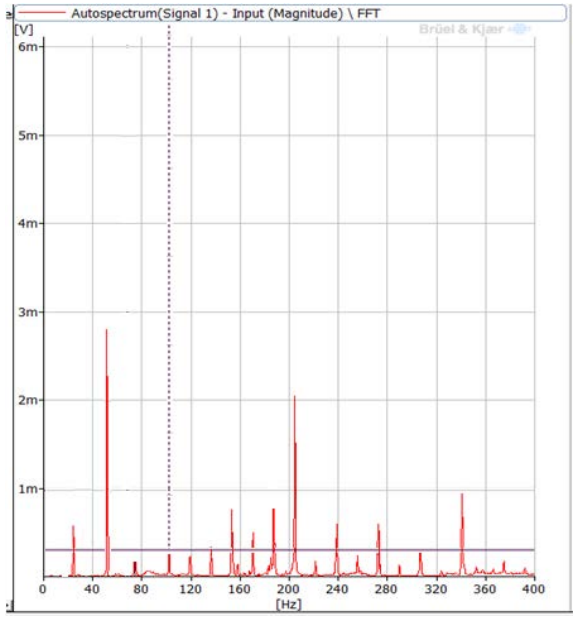

Figure 20. Vibration spectrum. Healthy machine, balanced currents

In a second case where the faulty machine supplied by the same sine three phase current system at 1500rpm-50Hz and 2A peak value, the FFT of the measured tangential vibration is presented in Figure 21. It can be observed the appearance of the spectral line at 100Hz (4.7mV delevired by the accelerometer).

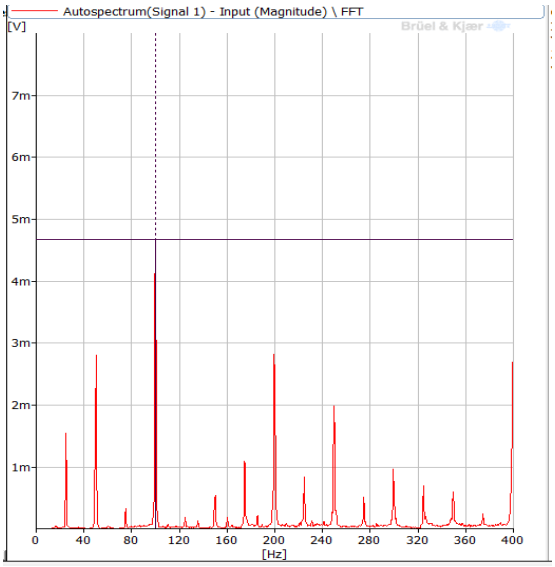

Figure 21. Vibration spectrum. Faulty machine, balanced currents

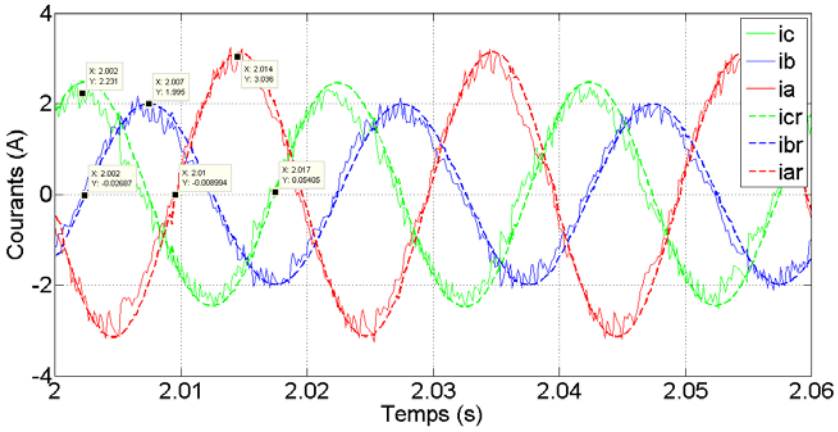

Figure 22. Corrected currents

In the third analyzed case, the supplied is changed to reduce the 100Hz harmonic of tangential vibrations. Actually, the magnitude of the direct component Id is still 2A and the magnitude and the phase of the inverse current Ii are adjusted in order to cancel the tangential vibration harmonic at 100Hz. For Ii=0.6A peak value, one obtain the three phase current in Figure 22 (in dashed line: the reference delivered

by simulink, in continuous line: the measured currents), and the tangential vibration FFT in Figure 23. One can observe the quasi-cancellation of the harmonic at 100Hz. The accelerometer provides a magnitude of 0.16mV that is twice lower than the value at the presumed healthy state, what means that the correction principle is able to act on the residual components generated by other phenomenon (eccentricity, demagnetization, etc.). Compared with the theoretical analysis, the ratio (Ii/Id) was 0.37 in theory and is 0.3 experimentally, what can be consider as acceptable insofar as the measured variable is not the torque but the vibrations which is and indirect effect of the torque.

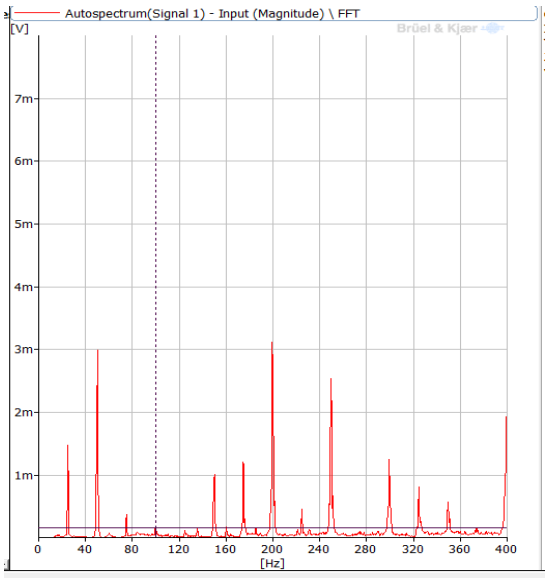

Figure 23. Vibration spectrum. Faulty machine, corrected currents

7. Conclusion

This paper proposes a model for a Surface Permanent Magnets Synchronous Motor (SPMSM) which allows simulating the torque ripple in healthy and faulty cases. As a solution for specific applications, it also gives the current references which can be used for supplying each motor phase in order to decrease the torque variation that occurs in faulty case. The results obtained from the developed model bring to the fore the link between the presence of the stator inter-turn short circuit fault in the motor and the torque ripple. It is shown that through a convenient control strategy applied in the motor phases which uses unbalanced currents; the torque ripple can decrease without affecting the operation of the machine. This principle is shown on a low power machine but it is still valid for higher power machine such as those used in automotive applications. Further work concerns the determination of

the inverse current directly from running operating conditions in faulty case and the application for a real practical system.

Bibliography

Abdel-Rady (2007). “A Newly Designed Instantaneous-Torque Control of Direct-Drive PMSM Servo Actuator with Improved Torque Estimation and Control Characteristics”. *IEEE Trans. Ind. Electron.*, vol. 54, p. 2864-2873, october.

Bahri *et al.* (2014). “Minimization of Torque Ripple Caused by a Stator Winding Dissymmetry in a Surface Permanent Magnet Synchronous Machine (SPMSM)”. ICEM 2014, Berlin, Germany, 2-5 September, p. 221-226.

Bahri E., Belkhayat D., Romary R., Pusca R. (2016). “Active control of torque ripple in a faulty surface permanent magnet synchronous motor. Case of stator inter-turn short circuit”. *Conférence Internationale en Sciences et Technologies Electriques au Maghreb, CISTEM 2016*, 26-28 octobre, Marrakech, Maroc.

Bahri *et al*. (2017). *A new approach for torque ripple reduction in a faulty Surface Permanent Magnet Synchronous Motor by inverse current injection*. Springer, Electrical Engineering, vol. 100, n° 2, june 2018, p. 565-579

Borghi C.A., Casadei D., Fabbri M., Serra G. (1998). “Reduction of the Torque Ripple in Permanent Magnet Actuators by a Multi-Objective Minimization Technique”, *IEEE Trans. Magnetics*, vol. 34, p. 2869-2872, september.

Ebrahimi and Faiz (2012). “Configuration impact on eccentricity fault detection in permanent magnet synchronous motors”, *IEEE Trans. Magnetics*, 48, p. 903-906

Ebrahimi *et al.* (2014). “Advanced eccentricity fault recognition in permanent magnet synchronous motors using stator current signature analysis”, *IEEE Trans. Ind.Electron*. 61, p. 2041-2052

Favre, Cardoletti and Jufer (1993). “Permanent-magnet synchronous motors: a comprehensive approach to cogging torque suppression”, I*EEE. Trans. Ind. Appl*, vol. 29, p. 1141-1149, november/december.

Hamiti *et al*. (2010). “Modeling of a synchronous reluctance machine accounting for space harmonics in view of torque ripple minimization” *Mathematics and Computers in Simulation*, vol. 81, p. 354-366.

Holtz and Springob (1996). “Identification and compensation of torque ripple in high-precision permanent magnet motor drives”, *IEEE Trans. Ind. Electro*n, vol. 43, p. 309-320, April.

Jeong, Byong and Nam (2013). “Dynamic Modeling and Control for SPMSMs With Internal Turn Short Fault” IEEE Trans Power electronics, vol. 28, p. 3495-3508, July.

Li, Xia and Zhou (2012). “Disturbance rejection control method for permanent magnet synchronous motor speed-regulation system”, *Mechatronics*, vol. 22, p. 706-714.

Mademlis and Margaris (2002). “Loss Minimization in Vector-Controlled Interior Permanent-Magnet Synchronous Motor Drives”, *IEEE Trans. Ind.Electron*. vol. 49, p. 1344-1347, december.

Pellegrino *et al*. (2010). "Core Losses and Torque Ripple in IPM Machines: Dedicated Modeling and Design Tradeoff", *IEEE. Trans. Ind. Applications* vol. 46, p. 2381-2391, November/December.

Tallam, Habetler and Harley (2002). "Transient Model for Induction Machines With Stator Winding Turn Faults", *IEEE. Trans. Ind. Appl*, vol. 38 p. 632-637, May/June.

Urresty *et al*. (2013). "Shaft trajectory analysis in a partially demagnetized permanent-magnet synchronous motor", *IEEE Trans. Ind.Electron*. 60: p. 3454-3461

Vaseghi B., Nahid-mobarakh B., Takorabet N., Meibody-Tabar F. (2011). "Inductance Identification and Study of PM Motor With Winding Turn Short Circuit Fault", *IEEE Trans. Magnetics*, vol. 47, p. 978- 981, May.

Appendix 1

Table.A.1. SPMSM parameter simulation

R(cm)	5	n_j^e	36	l_e^s (cm)	0.236	n(tr/min)	1500
L(cm)	17	N_t^s	36	f(Hz)	50	J	0.002
e(mm)	0.5	l_d^s (cm)	0.636	p	2	fr	0.0075

Appendix 2

Considering Figure 1 the fluxes through winding a, b, c generated by the stator are:

$$\begin{cases} \psi_{af} = L_{af}\left(i_a - i_f\right) + M_{afa2}i_a + M_{afb}i_b + M_{afc}i_c \\ \psi_{a2} = L_{a2}i_a + M_{afa2}\left(i_a - i_f\right) + M_{a2b}i_b + M_{a2c}i_c \\ \psi_b = M_{afb}\left(i_a - i_f\right) + M_{a2b}i_a + L_s i_b + M\ i_c \\ \psi_c = M_{afc}\left(i_a - i_f\right) + M_{a2c}i_a + L_s i_c + M\ i_b \end{cases} \quad (1a)$$

with M= -Ls/2, $M_{afb}=M_{afc}=kM$, $M_{a2b}=M_{a2c}=$ (1-k)M, and $M_{afa2}=k(1-k)Ls$. Considering that $\psi_a=\psi_{af}+\psi_{a2}$, the relation 1.a can be expressed as:

$$\begin{cases} \psi_a = \left(L_{af} + L_{a2} + 2M_{afa2}\right)i_a + \left(M_{afb} + M_{a2b}\right)i_b \\ +\left(M_{afc} + M_{a2c}\right)i_c - \left(M_{afa2} + L_{af}\right)i_f \\ \psi_b = \left(M_{afb} + M_{a2b}\right)i_a + L_s i_b + M\ i_c - M_{afb}i_f \\ \psi_c = \left(M_{afc} + M_{a2c}\right)i_a + M\ i_b + L_s i_c - M_{afc}i_f \\ \psi_{af} = \left(L_{af} + M_{afa2}\right)i_a + M_{afb}i_b + M_{afc}i_c - L_{af}i_f \end{cases} \quad (1b)$$

with $L_{af}=k^2L_s$, $L_{a2}=(1-k)^2L_s$. Taking in consideration that $L_{af}+L_{a2}+2M_{afa2}= k^2L_s+ (1-k)^2L_s+2k(1-k)L_s =L_s$, the relationship 1.b is given by following expression:

$$\begin{cases} \psi_a = L_s i_a + M i_b + M i_c - \left(L_{af} + M_{afa2}\right) i_f \\ \psi_b = M i_a + L_s i_b + M\ i_c - M_{afb} i_f \\ \psi_c = M i_a + M\ i_b + L_s i_c - M_{afc} i_f \\ \psi_{af} = \left(L_{af} + M_{afa2}\right) i_a + M_{afb} i_b + M_{afc} i_c - L_{af} i_f \end{cases} \tag{1c}$$

In the circuit presented in Figure 1 in the faulty machine the stator voltages are given by:

$$\begin{cases} V_{aN} = R_{af}\left(i_a - i_f\right) + R_{a2} i_a + \dfrac{d\Psi_a}{dt} + \dfrac{d\Psi_{ra}}{dt} \\ V_{bN} = R_s i_b + \dfrac{d\Psi_b}{dt} + \dfrac{d\Psi_{rb}}{dt} \\ V_{cN} = R_s i_c + \dfrac{d\Psi_c}{dt} + \dfrac{d\Psi_{rc}}{dt} \\ i_a + i_b + i_c = 0 \end{cases} \tag{2a}$$

Considering Rs=Raf+Ra2 and 1c the 2a is expressed as:

$$\begin{cases} V_{aN} = R_s i_a - R_{af} i_f + \dfrac{d\Psi_{ra}}{dt} + L_s \dfrac{di_a}{dt} + M \dfrac{di_b}{dt} + M \dfrac{di_c}{dt} + (-L_{af} - M_{afa2}) \dfrac{di_f}{dt} \\ V_{bN} = R_s i_b + \dfrac{d\Psi_{rb}}{dt} + M \dfrac{di_a}{dt} + L_s \dfrac{di_b}{dt} + M \dfrac{di_c}{dt} - M_{afb} \dfrac{di_f}{dt} \\ V_{cN} = R_s i_c + \dfrac{d\Psi_{rc}}{dt} + M \dfrac{di_a}{dt} + M \dfrac{di_b}{dt} + L_s \dfrac{di_c}{dt} - M_{afc} \dfrac{di_f}{dt} \\ 0 = -R_{af} i_a + (R_f + R_{af}) i_f - \dfrac{d\Psi_{raf}}{dt} + (L_{af} + M_{afa2}) \dfrac{di_a}{dt} + M_{afb} \dfrac{di_b}{dt} \\ + M_{afc} \dfrac{di_c}{dt} - L_{af} \dfrac{di_f}{dt} \end{cases} \tag{2b}$$